

Article

Synthetic NaX Zeolite as a Very Efficient Heavy Metals Sorbent in Batch and Dynamic Conditions

Zeinab Ezzeddine ^{1,2,*}, Isabelle Batonneau-Gener ¹, Yannick Pouilloux ¹, Hussein Hamad ² and Zeinab Saad ²

¹ Institut de chimie des milieux et matériaux de Poitiers (IC2MP)—UMR 7285, Poitiers University, 86000 Poitiers, France; isabelle.gener@univ-poitiers.fr (I.B.-G.); yannick.pouilloux@univ-poitiers.fr (Y.P.)

² Platform for Research and Analysis in Environmental Sciences, Lebanese University, P.O. Box 6573/14 Beirut, Lebanon; hussein.hamad@ul.edu.lb (H.H.); zsaad@ul.edu.lb (Z.S.)

* Correspondence: zeinab.ezzeddine@univ-poitiers.fr

Received: 10 May 2018; Accepted: 20 May 2018; Published: 24 May 2018



Abstract: The heavy metals removal efficiency of synthetic NaX zeolite has been studied. The sorbent was fully characterized by nitrogen sorption, X-ray diffraction, FT-IR and scanning electron microscopy. The batch sorption tests were performed taking into consideration several factors such as m/V ratio, contact time, pH and initial metal ions concentration. The maximum sorption capacities were 3.45, 3.86 and 4 mmol g⁻¹ for Pb²⁺, Cd²⁺ and Cu²⁺, respectively. Fixed-bed experiments were carried out to test the applicability of NaX zeolite as well as column regeneration experiments.

Keywords: NaX zeolite; heavy metals; adsorption; dynamic conditions

1. Introduction

Industrial evolution during the last decades has been beneficial in many aspects but it is also responsible for environmental pollution since many industrial effluents have been directly discharged in soil and natural water sources. Heavy metal pollution results mainly from mining operations, metal electroplating processes, battery manufacturing, tanneries and printing industries. Heavy metals are considered one of the most hazardous inorganic contaminants, since they are not biodegradable and can also accumulate in living organisms, causing various diseases. Lead, mercury, copper, cadmium, nickel and chromium are among the most common pollutants found in discharged industrial effluents [1]. Currently, many physico-chemical methods are available to remove heavy metal cations such as alkaline precipitation, ion exchange, membrane filtration and adsorption. Among them, adsorption is very attractive due to its simplicity, low cost and effectiveness. In order to develop efficient adsorbents, many studies have been carried out on many materials [2,3] such as polymer resins, natural zeolites, clays [4], bioadsorbents, activated carbon and organic-inorganic mesoporous silica. Zeolites are microporous crystalline aluminosilicates containing easily large amounts of extra framework cations. Thus, they have valuable exchange properties and are applied in water and wastewater treatment (water softening, heavy metal cation removal) [5]. Natural zeolites are widely used for these applications [6,7]. Nevertheless, these materials are not composed of pure zeolitic phases since they are generally mixed with quartz and other clay minerals. Furthermore, their chemical composition depends on their location [8,9]. Even though the cost of synthetic zeolites is higher, these materials have very reproducible and tunable physico-chemical properties. NaX Faujasite zeolite has a low Si/Al ratio (~1.18) which makes it more favorable for heavy metals sorption due to the presence of numerous exchangeable Na⁺ ions (6.54 mmol g⁻¹).

Despite of the huge number of studies dealing with heavy metals adsorption in literature using synthetic zeolites, there was no study done for comparing the efficiencies in batch and dynamic

conditions. The latter is very important in order to determine which material is more practical for wide range usage depending on the preparation cost together with the adsorption efficiency under several operation conditions. Based on this, the main objective of this paper is to study the behavior of NaX zeolite for heavy metals removal (Cu^{2+} , Cd^{2+} and Pb^{2+}) from water. Moreover, its performance in dynamic conditions was investigated as well since it is crucial for their applicability. Herein, the sorbent was used without post-synthesis treatment. Different factors that affect the sorption process were studied in batch and dynamic conditions. These include pH effect, mass effect, contact time, the presence of competitors' ions and the initial metal ions concentrations. The kinetics constants were established from treatment of the batch sorption results.

2. Materials and Methods

2.1. Materials

The synthetic NaX Faujasite ($\text{Na}_{88}\text{Al}_{88}\text{Si}_{104}\text{O}_{384}$) samples were purchased from IFP Energie Nouvelle (Rueil-Malmaison, France) and were used as received. Hydrochloric acid (HCl, 37%), sodium hydroxide (NaOH), copper nitrate ($\text{Cu}(\text{NO}_3)_2 \cdot 3\text{H}_2\text{O}$), cadmium nitrate ($\text{Cd}(\text{NO}_3)_2 \cdot 4\text{H}_2\text{O}$) and lead nitrate ($\text{Pb}(\text{NO}_3)_2$), were all purchased from Sigma Aldrich (St. Louis, MO, USA), and used as received. Ultrapure water was used throughout.

2.2. Characterization

The textural properties were determined by N_2 adsorption–desorption isotherms performed at $-196\text{ }^\circ\text{C}$ using Micromeritics ASAP 2010 (Micromeritics Instrument Corp., Norcross, GA, USA). All samples were out gassed under vacuum for at least 5 h at $350\text{ }^\circ\text{C}$ before measurement. Powder X-ray diffraction (XRD) patterns were recorded on an Empyrean X-ray diffractometer (Malvern Panalytical Ltd., Royston, UK) using $\text{Cu K}\alpha$ ($\lambda = 1.54\text{ \AA}$) radiation with a scanning rate of $0.008^\circ\text{ min}^{-1}$ from 3° to $70^\circ 2\theta$. The morphology of NaX zeolite was obtained by scanning electron microscopy (SEM, JEOL 7001 FEG, Tokyo, Japan). Thermogravimetric analysis (TG) was conducted in air from 25 to $900\text{ }^\circ\text{C}$ using SDT Q600 TA Instruments (New Castle, DE, USA). The functional groups were identified by Fourier Transform Infrared (FTIR) Spectroscopy in the range of $400\text{--}4000\text{ cm}^{-1}$. The samples were first mixed with KBr and then pressed into pellets and analyzed with FT-IR—6300 JASCO (Oklahoma city, OK, USA). The zeta potential of NaX was measured using a Zeta-Meter System 4.0 unit (Staunton, VA, USA), equipped with an electrophoresis cell (type GT-2) of 10 cm long and 4 mm in diameter with K factor and two platinum electrodes. The pH was adjusted by using hydrochloric acid or sodium hydroxide solution.

2.3. Batch Adsorption Experiments

Metal ions solutions (Cu^{2+} , Pb^{2+} and Cd^{2+}) were prepared from their corresponding nitrate salts in ultrapure water to obtain solutions of different concentrations. In typical batch studies, a weighed amount (m) of the solid powder was placed in a flask containing (V) mL of a metal solution of desired concentration. The (m)/(V) ratios depend on the nature of the adsorbent. The mass of material was varied between 10 mg and 60 mg in order to optimize the (m)/(V) ratio for batch adsorption experiments. The Cu^{2+} solution volumes were fixed to 100 mL. The flask was continuously stirred at $25\text{ }^\circ\text{C}$ at 300 rpm. At the end of each sorption experiment, the solution was filtered and the metal ion concentration was determined using Atomic Adsorption Spectrophotometer (AAS, Perkin Elmer AA200, Waltham, MA, USA). The same procedure was repeated for the three divalent metals used. The removal efficiency (% Adsorption) was calculated by Equation (1):

$$R = \frac{C_0 - C_t}{C_0} \times 100 \quad (1)$$

where C_0 and C_t are the heavy metal initial concentration and at time t concentrations. The sorption capacity (mmol g^{-1}) of the sorbent at equilibrium was calculated by Equation (2) where C_e is the concentration at equilibrium, (V) is the volume in L of metal solution and m is the mass in g of the adsorbent. Kinetic study was performed by studying the sorption as a function of time.

$$q_e = \frac{(C_0 - C_e)V}{m} \quad (2)$$

For obtaining the isotherms, the batch experiments were done with optimal (m)/(V) ratio for the NaX sorbent. The initial metal ions concentrations were varied between 0.17 mmol L^{-1} and 5 mmol L^{-1} . The solutions were stirred for 120 min at $25 \text{ }^\circ\text{C}$ then filtered by a $0.45 \text{ }\mu\text{m}$ syringe filter and the remaining metal ions were measured by AAS in order to calculate C_e and q_e . The effect of pH was studied by varying the solution pH in the range between 2 and 7.

2.4. Fixed Bed Column Studies

Although batch studies give information about the effectiveness and the sorption capacity of the sorbent, column operations are important for the practical utility design. The main advantage of fixed bed is that it allows a more efficient usage of the sorbent.

Experimental Set-Up

For fixed bed experiments, a stainless-steel column was used with a 100 mm length and a diameter of 4.6 mm. 0.1 g of each adsorbent was packed in the column separately. The polluted water mixture was fed into the column using in HPLC pump (Gilson 307, Middleton, WI, USA), with a constant flow rate of 1 mL min^{-1} . The eluted samples were collected then analyzed by atomic absorption spectrometry (AAS). The efficiency of the sorbent under dynamic operation conditions can be determined in terms of C/C_0 (C = effluent metal ions concentration and C_0 = influent metal ions concentration) as a function of time or volume of the eluate for a given bed height (breakthrough curve). The column capacity, $q_{e(\text{exp})}$ (mmol g^{-1}), for a given feed concentration and flow rate is calculated by integrating the surface area below the breakthrough curve according Equation (3):

$$q_{e(\text{exp})} = \frac{C_0}{m} \int_0^{V_e} \left(1 - \frac{C}{C_0}\right) dv \quad (3)$$

Fixed bed experiments were also performed in order to test the applicability of NaX zeolite. The water samples were spiked with an equimolar concentration of metal ions (0.47 mmol L^{-1}). Elution of adsorbed ions was accomplished by 1 M NaCl solution at flow rate 1 mL min^{-1} .

3. Results and Discussion

3.1. Physico-Chemical Characterizations

The obtained XRD pattern for NaX zeolite is shown on Figure 1a. The sharp peaks in the 2θ ranges of 3° – 35° indicate that the microporous structure of zeolite is well crystallized. The Na-X phase was identified on the basis of a group of characteristics for their reflections ($d = 14.47, 3.81, 5.73, 8.85, 4.42, 7.54, 4.81, 3.94$) [10]. The detailed JCPDS pattern lines for NaX zeolite are already mentioned in literature [11]. Scanning electronic micrographs show the crystallites of NaX forming fine cubic particles with an average size $3 \text{ }\mu\text{m}$ (Figure 1b). The nitrogen adsorption–desorption isotherms for NaX are shown in Figure 2a. The adsorption isotherm is of type I which is characteristic of a microporous material. No important increase of N_2 adsorbed amount is noticed for high P/P_0 values indicating the absence of mesopores and external surface. The BET surface area is $745 \text{ m}^2 \text{ g}^{-1}$ and the microporous volume estimated from t-plot is $0.317 \text{ cm}^3 \text{ g}^{-1}$. Thermogravimetric analysis (TGA) was used to verify the absence of organic template and to estimate the zeolite water content. The obtained signals recorded under air flow are shown on Figure 2b. The weight loss observed between

25 °C and 900 °C is attributed to the desorption of the physisorbed water molecules from the zeolite cavities. The desorbed water amount is estimated to be 26%. This high amount results from the strong hydrophilicity of NaX zeolite due to its low Si/Al ratio. NaX zeolite FT-IR spectrum is shown in Figure 3a. The bands at 1200–450 cm^{-1} are assigned to Si–O–Al, Si–O–Si, Si–O and Al–O species [12]. The band at 660 cm^{-1} is characteristic to Si–O–Me where Me is the exchangeable Na^+ ion. Vibrations of Na^+ cations against the framework occur in the far infrared region (200–500 cm^{-1}). The variation of the surface charge of NaX zeolite as a function of pH is shown in Figure 3b. As the pH increase the zeta potential of NaX decrease and the point of zero charge pH_{zpc} was found to be 4.7 so the surface has more negative charge above pH 4.7 which increase heavy metals cations adsorption above this pH value.

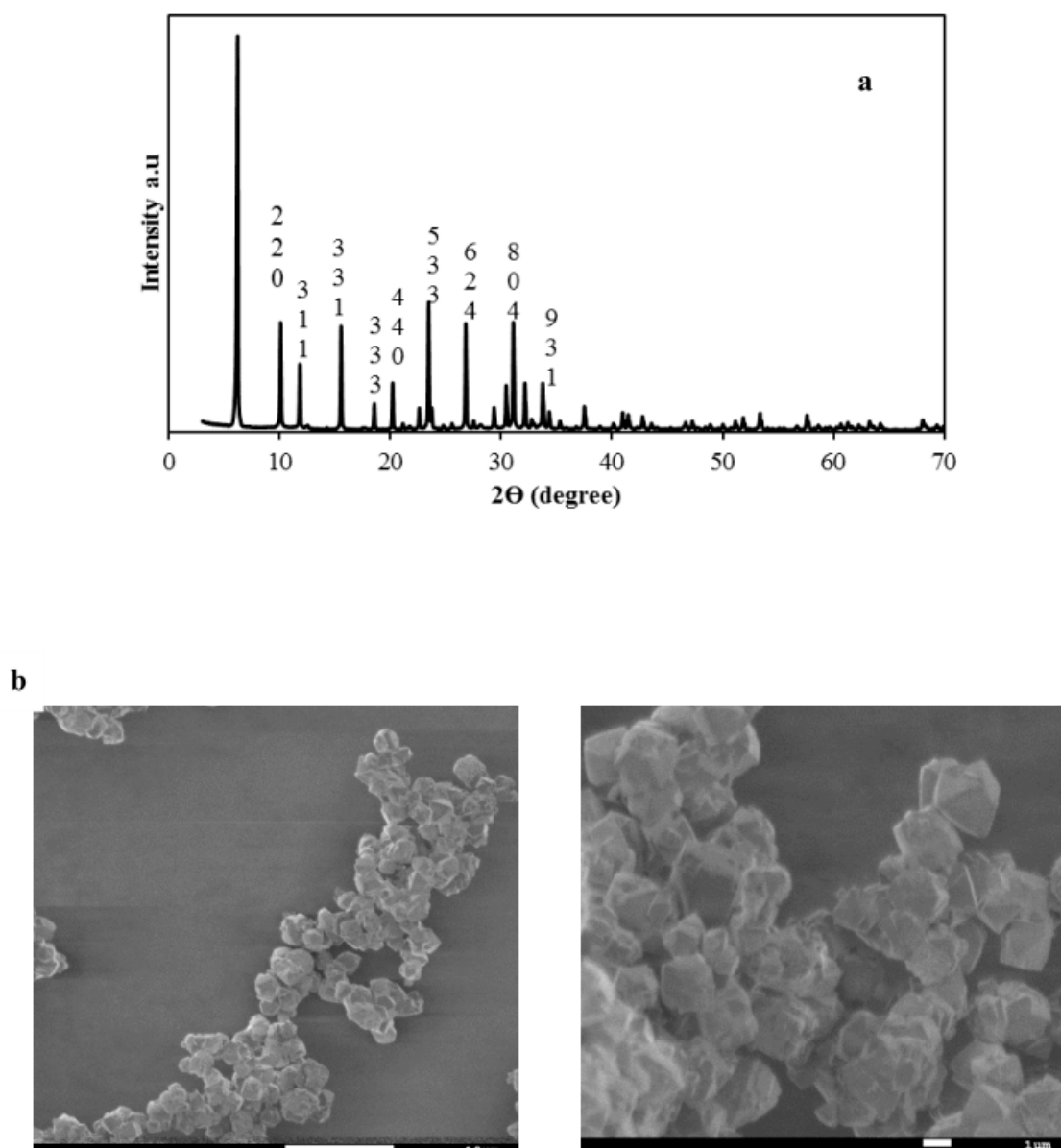


Figure 1. XRD patterns of NaX zeolite (a) and scanning electron microscopy (b).

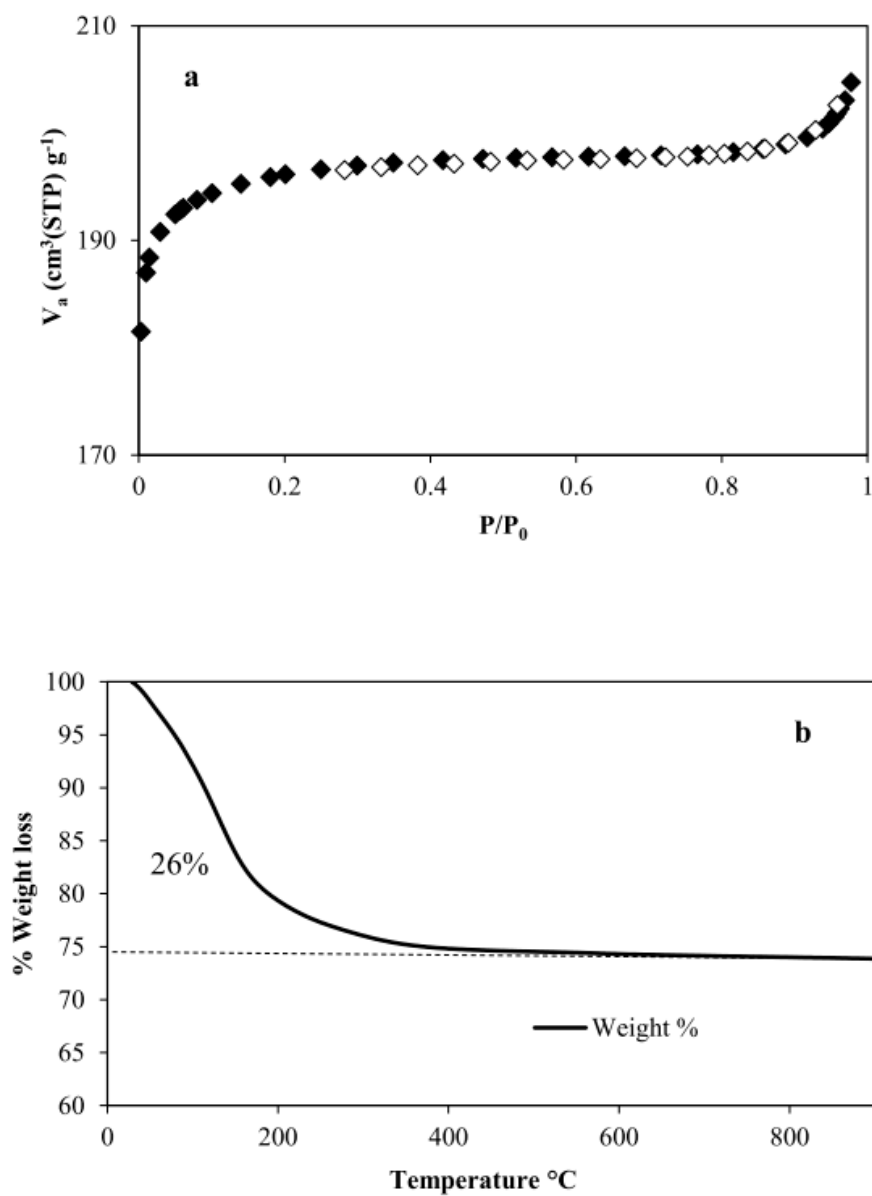


Figure 2. N₂ adsorption-desorption isotherms (adsorption in black and desorption in white) of NaX zeolite (a) and thermogravimetric analysis (b).

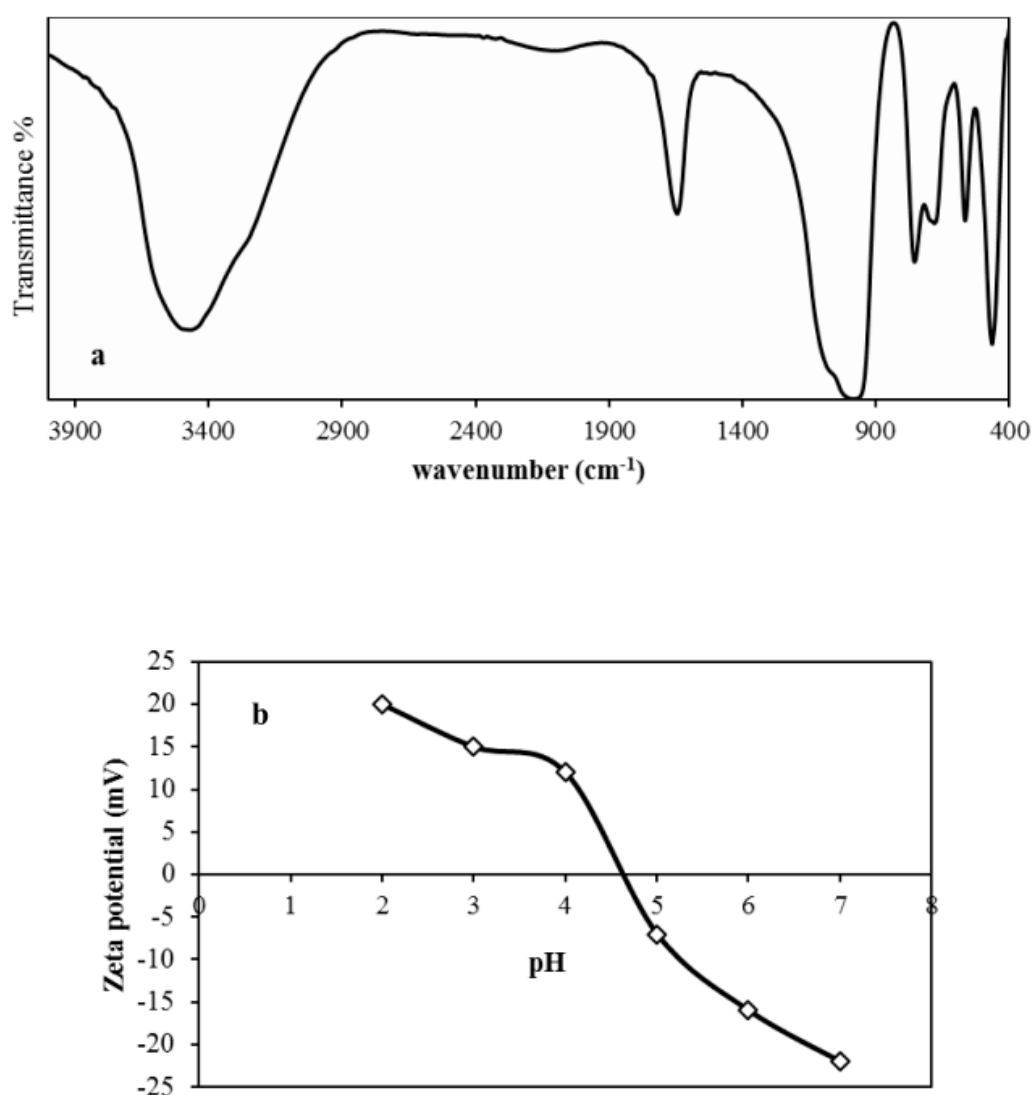


Figure 3. FT-IR spectra for NaX zeolite (a) and the pH of zero-point charge (pHzpc) (b).

3.2. Batch Adsorption Experiments

3.2.1. Mass Effect

Figure 4 shows the (m)/(V) ratio effect on Cu²⁺ removal from aqueous solution. For NaX zeolite, below 0.3 mg mL⁻¹, the sorption percentage increases when the (m)/(V) ratio increases. This is due to the increase in the amount exchangeable sites. Above 0.3 mg mL⁻¹, (m)/(V) ratio increase has no effect since the sorption reaches nearly 100%. From this result, a zeolite mass of 20 mg was found to be the more suitable so all the following experiments which were done with a ratio (m)/(V) = 0.2 (mg mL⁻¹). The (m)/(V) ratio depends on the type of zeolite used, for example Nibou et al. used also synthetic NaX zeolite and they used 250 mg for 100 mL of metal solution [9]. Erdem et al. worked with clinoptilolite (natural zeolite) where they used 10 g of solid for 500 mL of metal solution [13]. Another study was performed by Hui et al. with 100 mg of synthetic zeolite 4A for 100 mL metal ions solution [14].

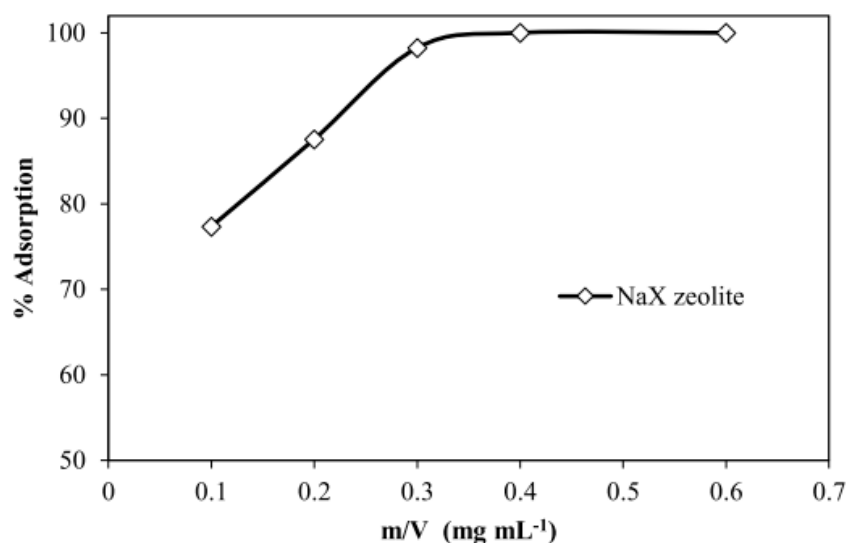


Figure 4. Effect of (m)/(V) on Cu^{2+} adsorption on NaX zeolite (pH = 5.8, t = 2 h at 25 °C and $[\text{Cu}^{2+}]_i = 0.47 \text{ mmol L}^{-1}$).

3.2.2. pH Effect

The solution pH is an important factor that affects metal ions sorption since it controls metal ions speciation as well as the surface charge of the sorbent. Figure 5 shows the adsorption of Cu^{2+} , Cd^{2+} and Pb^{2+} on NaX for different pH values. As the pH increases from 2 to 5, adsorption increases for all metal ions since $\text{pH}_{\text{zpc}} = 4.7$ so adsorption will reach its maximum capacity above this value. Furthermore, NaX zeolite structure is not stable in strongly acidic media (dealumination).

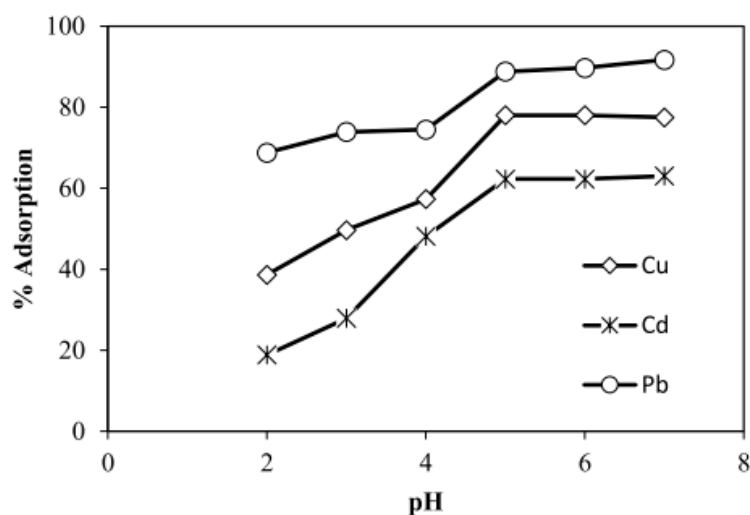


Figure 5. Effect of pH on the adsorption of metal ions on NaX zeolite (t = 2 h at 25 °C and $[\text{M}^{2+}]_i = 0.47 \text{ mmol L}^{-1}$).

3.2.3. Kinetics Study

The metal cation adsorbed quantities were monitored as a function of time. The experimental data were presented in Figure 6. For all heavy metal cations, equilibrium was reached in the first 20 min which indicates the rapid exchange between Na^+ ions of NaX zeolite and the heavy metal cations. The obtained experimental data were fitted by two kinetic models, pseudo first order (Equation

(4) [15] and pseudo second order (Equation (5)) [16] in order to determine the reaction order and the kinetics constants.

$$\ln(q_e - q_t) = \ln q_e - k_1 t \quad (4)$$

$$q_t = \frac{k_2 q_e^2 t}{1 + k_2 q_e t} \quad (5)$$

where q_t and q_e are the amounts of metal ions adsorbed (mmol g^{-1}) at time t (min) and at equilibrium respectively, and k_1 is the rate constant of adsorption (min^{-1}) and k_2 is the pseudo-second order rate constant ($\text{g mmol}^{-1} \text{min}^{-1}$), The initial sorption rates ($h = k_2 q_e^2$) expressed in $\text{mmol g}^{-1} \text{min}^{-1}$ were also calculated.

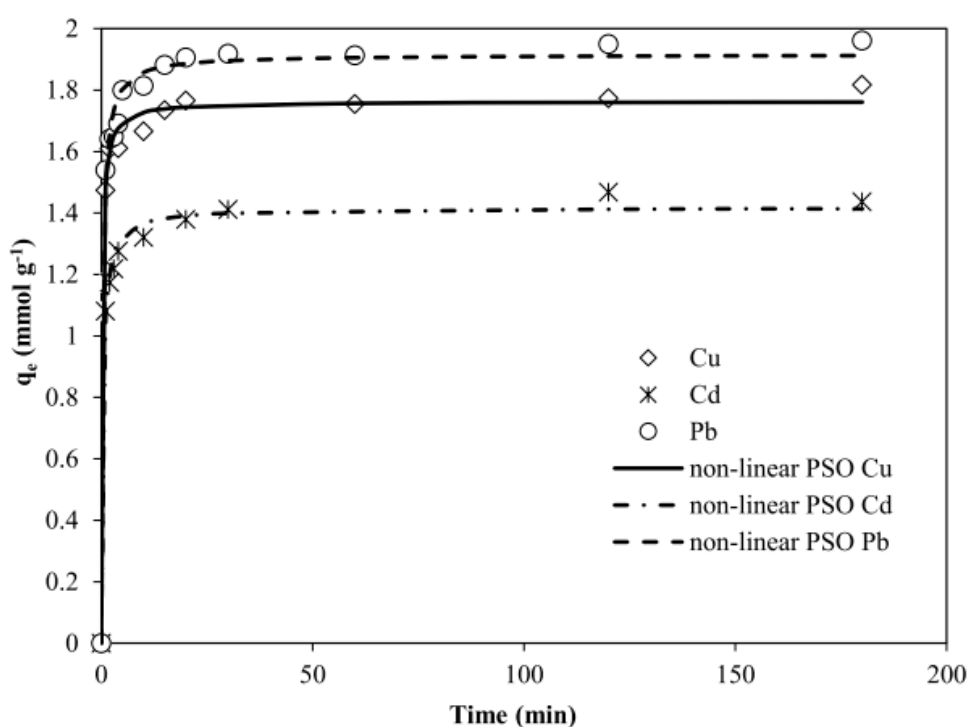


Figure 6. Non-linear pseudo-second-order kinetic models for M^{2+} adsorption on NaX zeolite (pH = 5.8 at 25 °C and $[Me^{2+}]_i = 0.47 \text{ mmol L}^{-1}$).

The kinetic data for NaX zeolite are presented in Table 1 and the fit in Figure 6. The obtained correlation coefficients of the pseudo-second-order model are higher than those of pseudo-first-order model. Also, the equilibrium capacities (q_e values) calculated from the pseudo-second-order are closer to the experimental values. From these results, it can be concluded that the sorption of the metal ions (Cu^{2+} , Cd^{2+} and Pb^{2+}) follows the pseudo-second-order model which means that adsorption might be the rate limiting step involving valence forces either through sharing or exchange of electrons between adsorbent and metal ions [17]. Concerning the adsorption rate h , it was found to be in the following order: $\text{Pb}^{2+} > \text{Cu}^{2+} > \text{Cd}^{2+}$ which means that the adsorbents are more selective for Pb^{2+} and Cu^{2+} than for Cd^{2+} . These findings prove that the selectivity of the sorbent is directly related to the nature of the metals [18] while the adsorption capacity is only influenced by the number of sorption or exchangeable sites.

Table 1. Comparison of the first and the second order kinetic models for NaX zeolite.

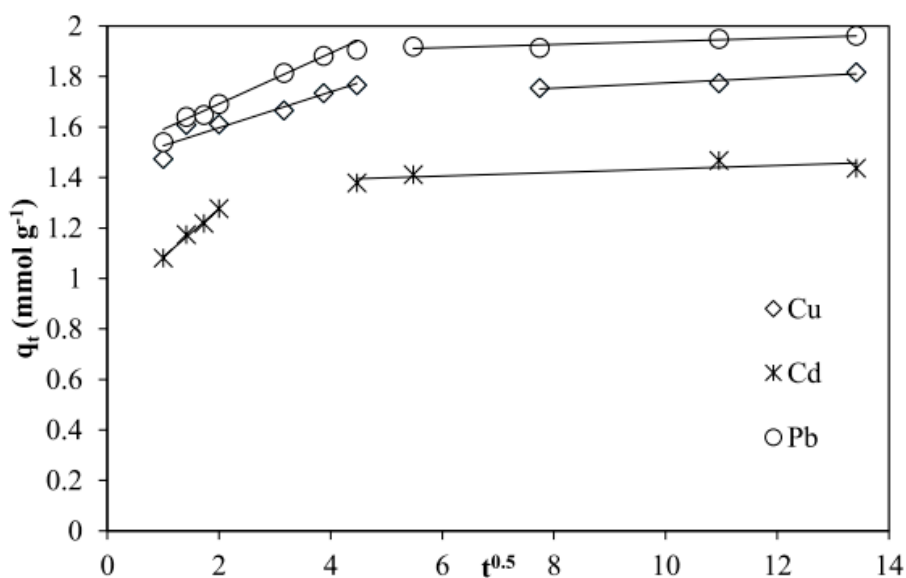
NaX Zeolite								
q_e^{exp} (mmol g ⁻¹)	First Order Kinetic Model				Second Order Kinetic Model			
	k_1 (min ⁻¹)	q_e^{cal} (mmol g ⁻¹)	R^2	k_2 (g mmol ⁻¹ min ⁻¹)	q_e^{cal} (mmol g ⁻¹)	h (mmol g ⁻¹ min ⁻¹)	R^2	
Cu ²⁺	1.82	0.7	1.69	0.935	0.90	1.8	2.94	0.997
Cd ²⁺	1.54	1	1.35	0.978	1.19	1.45	2.52	0.996
Pb ²⁺	1.96	1	1.8	0.972	0.79	1.96	3.04	0.999

3.2.4. Intra-Particle Diffusion Model

The intra-particle diffusion model was used to analyze the kinetic results in order to determine whether it is the rate-limiting step in the sorption process. The intra-particle diffusion model is expressed in Equation (6):

$$q_t = k_{id}t^{1/2} + C \quad (6)$$

where k_{id} is the intra-particle diffusion rate constant (mg g⁻¹ min^{-1/2}); C is the intercept (mg g⁻¹). If the plot of the amount of metal ions adsorbed (q_t) versus $t^{1/2}$ is linear and passes through the origin, then intra-particle diffusion is the only rate-controlling step [19]. The results are illustrated in Figure 7 and the parameters in Table 2.

**Figure 7.** Intraparticle diffusion model for NaX zeolite.**Table 2.** Parameters of intra-particle diffusion model for NaX zeolite.

	k_{id1} (mmol/g min ^{1/2})	C_1	R^2	k_{id2} (mmol/g min ^{1/2})	C_2	R^2
Cu ²⁺	0.141	2.91	0.891	0.021	3.34	0.913
Cd ²⁺	0.209	2.04	0.844	0.014	2.73	0.64
Pb ²⁺	0.2	2.98	0.903	0.012	3.75	0.873

It was found that the plot q_t versus $t^{0.5}$ is not a straight line passing through the origin so the sorption process is not controlled by the intra-particle diffusion at all.

3.3. Adsorption Isotherms

3.3.1. Langmuir Isotherm Model

Langmuir Isotherm is a model that assumes monolayer coverage of a finite number of identical sites present on the surface such that no further adsorption takes place. The isotherm can be modeled by Langmuir Equation (7) [20]:

$$q_e = \frac{K_L \times q_{\max} C_e}{1 + K_L C_e} \quad (7)$$

q_{\max} is the maximum sorption capacity (monolayer coverage, mmol g⁻¹), i and K_L is Langmuir isotherm constant (g mmol⁻¹).

3.3.2. Freundlich Isotherm Model

This model describes the non-ideal and reversible adsorption, not limited to monolayer formation. It can be applied to multilayer sorption, with non-uniform distribution of sorption heat and affinities over a heterogeneous surface [21]. The isotherm is expressed by Equation (8):

$$q_e = K_f C_e^{1/n} \quad (8)$$

where K_f is Freundlich isotherm constant (mmol g⁻¹) and n is the adsorption intensity. The Langmuir and Freundlich adsorption isotherms for NaX zeolite are shown in Figure 8 and the corresponding parameters are listed in Table 3. From these results it can be concluded that the experimental data are best fitted by Langmuir. These isotherms are L shape in Giles classification [22] and exhibit a sharp initial slope indicating that the material is very efficient at low metal concentrations. Then, a plateau is observed indicating that the maximal sorbent capacity is reached. The zeolite has higher affinity for Pb²⁺ and Cu²⁺ than for Cd²⁺. The theoretical exchange capacity was calculated from the NaX zeolite unit cell formula (Na₈₈Al₈₈Si₁₀₄O₃₈₄). 1 g of NaX zeolite contains 6.54 mmol of Na⁺ ions so theoretically, it has a maximum adsorption capacity for divalent ions equal to 3.27 mmol g⁻¹. The q_{\max} values obtained from Langmuir isotherms fit are in accordance with theoretical exchange capacity except for Cu²⁺ (Table 3). The elevated exchange capacity is due to copper II speciation at pH 5.8. For this pH value, CuOH⁺ species will be also present. In this case only one Na⁺ ion is exchanged by one CuOH⁺ resulting in an increase of the zeolite copper capacity to 4.0 mmol g⁻¹. The dominant species for the other two metals will be in the form M²⁺ and the maximum sorption capacity obtained for Pb²⁺ and Cd²⁺ (3.2 and 3.1 mmol g⁻¹ respectively) are very close to the theoretical divalent metal cation exchange capacity. It is worth mentioning that the obtained capacities in this study are higher than those obtained elsewhere with other types of sorbents [23–25].

Table 3. Langmuir and Freundlich parameters for NaX zeolite adsorption isotherms.

Metal	Langmuir			Freundlich		
	q_{\max} (mmol g ⁻¹)	K_L (L mmol ⁻¹)	R^2	n	K_f (L g ⁻¹)	R^2
Cu ²⁺	4.0	57.7	0.991	5	4.5	0.738
Cd ²⁺	3.1	23.7	0.988	2.2	5.2	0.842
Pb ²⁺	3.2	52.0	0.991	5.3	3.4	0.860

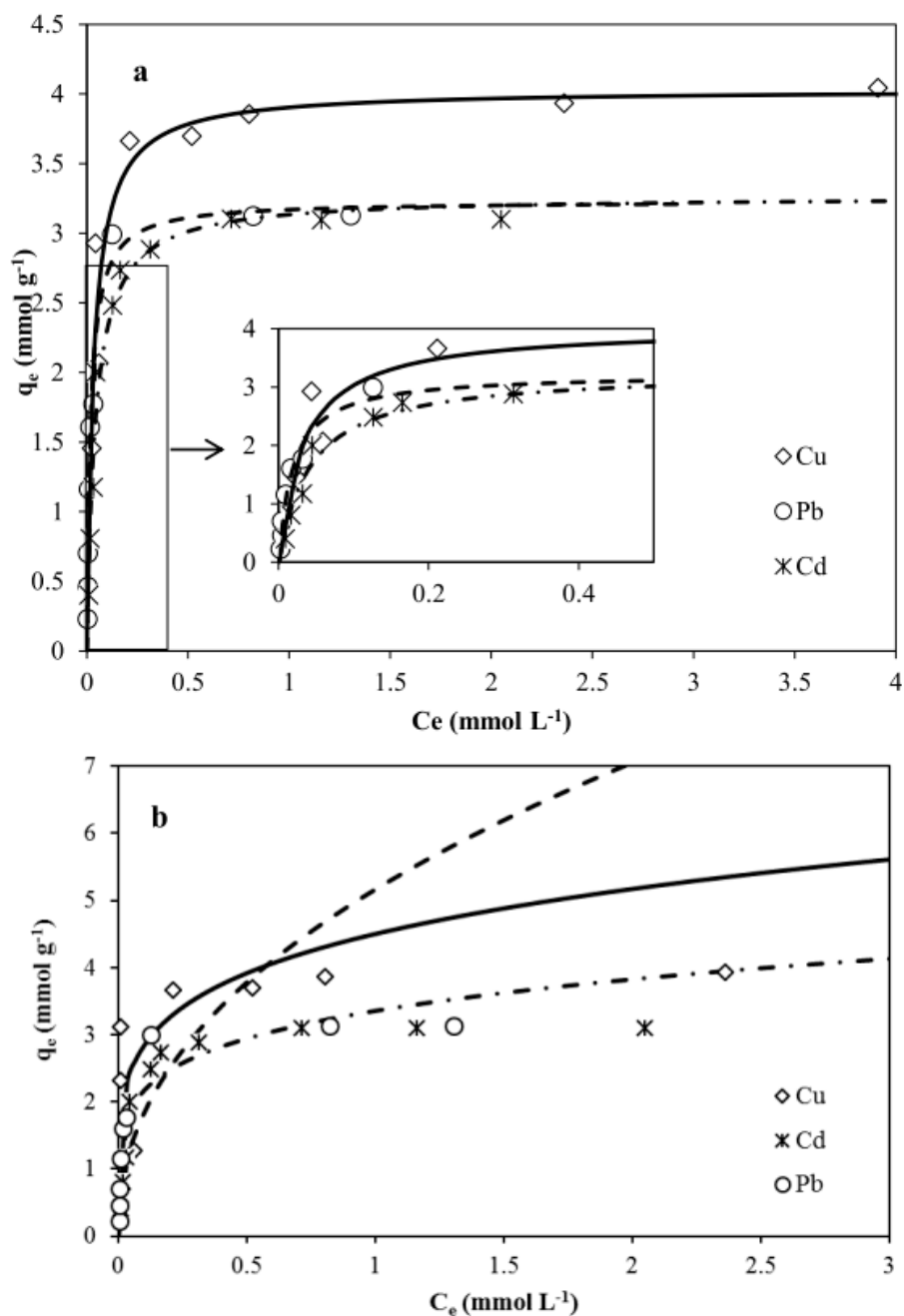


Figure 8. Experimental Cu²⁺, Cd²⁺, Pb²⁺ adsorption isotherms on NaX (open symbols) and their corresponding Langmuir (a) and Freundlich (b) modeled isotherms (lines).

3.4. Breakthrough Curves

Fixed bed column experiments were also studied in order to test the applicability of NaX zeolites for heavy metals removal on a large scale. The experiments were done using a mixed equimolar metal ions solution in ultra-pure water. The obtained breakthrough curves are shown in Figure 9a. The curves show that saturation was reached after 700 mL of contaminated water was passed through the column. Furthermore, it was noticed that the adsorption behavior of Pb²⁺ ions was different from the other metal ions due to the high affinity of NaX zeolite towards it. The results are listed in Table 4. For comparison, the capacities obtained from batch experiment done with the same equimolar mixture of heavy metal cations are also reported in Table 4.

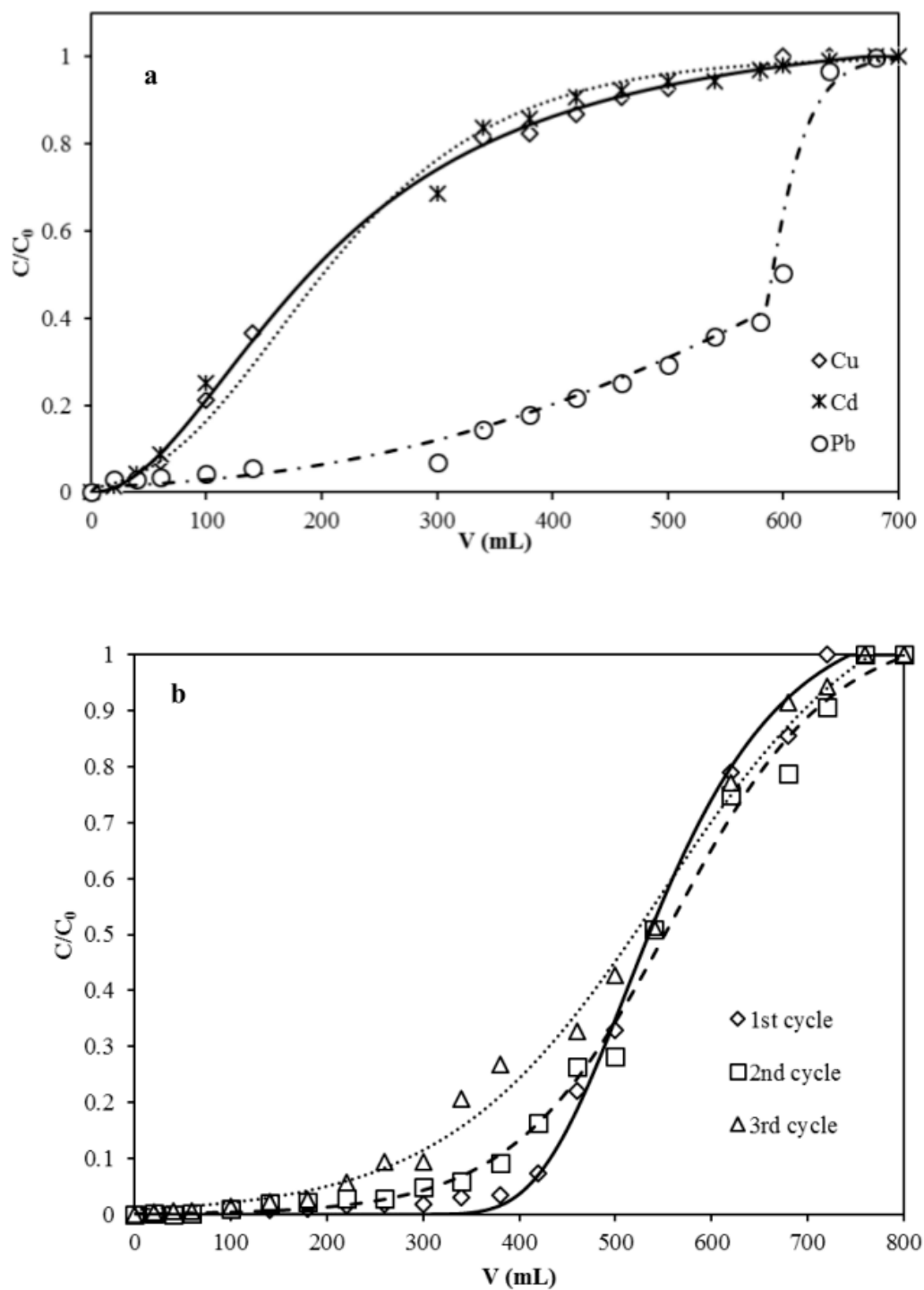


Figure 9. Breakthrough curves for Cu^{2+} , Cd^{2+} and Pb^{2+} adsorption on NaX (a) and for Cu^{2+} adsorption on NaX after regeneration (b) (pH = 5.8 at 25 °C $[M^{2+}]_i = 0.47$ mmol L⁻¹, m = 100 MG, flow rate 1 mL min⁻¹).

Table 4. Column capacity for Cu²⁺, Ni²⁺, Cd²⁺ and Pb²⁺ adsorption on NaX zeolite.

Metal Ion	Batch Capacity (mmol g ⁻¹)	Column Capacity (mmol g ⁻¹)
Cu ²⁺	1.02	0.960
Cd ²⁺	1	0.867
Pb ²⁺	2.21	2.23

3.5. Column Regeneration

Column regeneration is important for its reusability, so sorption-desorption tests were done for Cu²⁺ as an example. Then the regeneration efficiency was evaluated by performing two more sorption cycles using the same column and regenerating it after each cycle (Table 5). The three obtained curves are shown in Figure 9b.

Table 5. Regeneration efficiency after three Cu²⁺ adsorption–desorption cycles.

	Capacity (mmol g ⁻¹)	Regeneration Efficiency (%)
1st cycle	2.43	-
2nd cycle	2.36	97.1
3rd cycle	2.24	92.2

After three consecutive Cu²⁺ adsorption–desorption cycles, the NaX zeolite packed column conserved up to 92% of its original capacity which means that it can be used several times. Also, the high efficiency conserved after regeneration proves that heavy metals can be successfully elute without degrading the structure of the adsorbent. Further regeneration could be done using mixed equimolar metal ions solution.

4. Conclusions

Synthetic NaX zeolite was used for heavy metals removal. Its sorption efficiency to eliminate Cu²⁺, Cd²⁺ and Pb²⁺ from water was investigated. The obtained sorption capacities were high for all metals. Cu²⁺ speciation as a function of pH is the reason behind its elevated sorption capacity compared to Cd²⁺ and Pb²⁺. The kinetic data were well fitted by the pseudo second order and the maximum sorption capacities were calculated from Langmuir isotherms. Concerning continuous flow studies, NaX zeolite was efficient in column experiments as well and it conserved 92% of its sorption capacity after two successive regeneration cycles.

Author Contributions: I.B.-G. conceived the work; Z.E. designed the experiments and performed the experiments; Z.E., I.B.-G. and Y.P. analyzed and interpreted the data; Z.E. wrote the manuscript, Y.P. managed the study and the unit research in Poitiers, H.H. and Z.S. Participated in the manuscript correction.

Acknowledgments: The authors are thankful to the (IC2MP) 'Institut de Chimie des Milieux et Matériaux de Poitiers—UMR 7285', Poitiers University, PRES and Lebanese University for the financial support of this work.

Conflicts of Interest: The authors declare no conflict of interest.

References

- Ahmaruzzaman, M. Industrial wastes as low-cost potential adsorbents for the treatment of wastewater laden with heavy metals. *Adv. Colloid Interface Sci.* **2011**, *166*, 36–59. [[CrossRef](#)] [[PubMed](#)]
- Babel, S.; Kurniawan, T.A. Low-cost adsorbents for heavy metals uptake from contaminated water: A review. *J. Hazard. Mater.* **2003**, *97*, 219–243. [[CrossRef](#)]
- Bailey, S.E.; Olin, T.J.; Bricka, R.M.; Adrian, D.D. A review of potentially low-cost sorbents for heavy metals. *Water Res.* **1999**, *33*, 2469–2479. [[CrossRef](#)]
- Franus, M.; Bandura, L. Sorption of Heavy Metal Ions from Aqueous Solution by Glauconite. *Fresenius Environ. Bull.* **2014**, *23*, 825–839. [[CrossRef](#)]

5. Kesraoui-ouki, S.; Cheeseman, C.R.; Perry, R. Natural zeolite utilisation in pollution control: A review of applications to metals' effluents. *J. Chem. Technol. Biotechnol.* **1994**, *59*, 121–126. [[CrossRef](#)]
6. Athanasiadis, K.; Helmreich, B. Influence of chemical conditioning on the ion exchange capacity and on kinetic of zinc uptake by clinoptilolite. *Water Res.* **2005**, *39*, 1527–1532. [[CrossRef](#)] [[PubMed](#)]
7. Bandura, L.; Franus, M.; Panek, R.; Wozuk, A.; Franus, W. Characterization of zeolites and their use as adsorbents of petroleum substances. *Przem. Chem.* **2015**, *3*, 323–327. [[CrossRef](#)]
8. Oter, O.; Akcay, H. Use of Natural Clinoptilolite to Improve Water Quality: Sorption and Selectivity Studies of Lead(II), Copper(II), Zinc(II), and Nickel(II). *Water Environ. Res.* **2007**, *79*, 329–335. [[CrossRef](#)] [[PubMed](#)]
9. Cincotti, A.; Mameli, A.; Locci, A.M.; Orru, R.; Cao, G. Heavy metals uptake by Sardinian natural zeolites: Experiment and modeling. *Ind. Eng. Chem. Res.* **2006**, *45*, 1074–1084. [[CrossRef](#)]
10. Franus, W. Characterization of X-type Zeolite Prepared from Coal Fly Ash. *Pol. J. Environ. Stud.* **2012**, *21*, 337–343.
11. Treacy, M.M.J.; Higgins, J.B. (Eds.) *Collection of Simulated XRD Powder Patterns for Zeolites*, Fourth Revised ed.; Elsevier: Amsterdam, The Netherlands, 2001.
12. Nibou, D.; Mekatel, H.; Amokranea, S.; Barkatb, M.; Trari, M. Adsorption of Zn²⁺ ions onto NaA and NaX zeolites: Kinetic, equilibrium and thermodynamic studies. *J. Hazard. Mater.* **2010**, *173*, 637–646. [[CrossRef](#)] [[PubMed](#)]
13. Erdem, E.; Karapinar, N.; Donat, R. The removal of heavy metal cations by natural zeolites. *J. Colloid Interface Sci.* **2004**, *280*, 309–314. [[CrossRef](#)] [[PubMed](#)]
14. Hui, K.S.; Chao, C.Y.H.; Kot, S.C. Removal of mixed heavy metal ions in wastewater by zeolite 4A and residual products from recycled coal fly ash. *J. Hazard. Mater.* **2005**, *127*, 89–101. [[CrossRef](#)] [[PubMed](#)]
15. Lagergren, S. Zur theorie der sogenannten adsorption gelöster stoffe, Kungligasvenska vetenskapsakademiens. *Handlingar* **1898**, *24*, 1–39.
16. Vasanth Kumar, K. Linear and non-linear regression analysis for the sorption kinetics of methylene blue onto activated carbon. *J. Hazard. Mater.* **2006**, *B137*, 1538–1544. [[CrossRef](#)] [[PubMed](#)]
17. Shavandi, M.A.; Haddadian, Z.; Ismail, M.H.S.; Abdullah, N.; Abidin, Z.Z. Removal of Fe(III), Mn(II) and Zn(II) from palm oil mill effluent (POME) by natural zeolite. *J. Taiwan Inst. Chem. Eng.* **2012**, *43*, 750–759. [[CrossRef](#)]
18. Ezzeddine, Z.; Batonneau-Gener, I.; Pouilloux, Y.; Hamad, H.; Saad, Z.; Kazpard, V. Divalent Heavy Metals Adsorption onto Different Types of EDTA-Modified Mesoporous Materials: Effectiveness and Complexation Rate. *Microporous Mesoporous Mater.* **2015**, *212*, 125–136. [[CrossRef](#)]
19. Ji, F.; Li, C.; Tang, B.; Xu, J.; Lu, G.; Liu, P. Preparation of cellulose acetate/zeolite composite fiber and its adsorption behavior for heavy metal ions in aqueous solution. *Chem. Eng. J.* **2012**, *209*, 325–333. [[CrossRef](#)]
20. Langmuir, I. The constitution and fundamental properties of solids and liquids. Part I. Solids. *J. Am. Chem. Soc.* **1916**, *38*, 2221–2295. [[CrossRef](#)]
21. Freundlich, H.M. Über die adsorption in losungen. *J. Phy. Chem.* **1906**, *57*, 385–471. [[CrossRef](#)]
22. Giles, C.; Smith, D.; Huitson, A. A general treatment and classification of the solute adsorption isotherm. I. Theoretical. *J. Colloid Interface Sci.* **1974**, *47*, 755–765. [[CrossRef](#)]
23. Tohdee, K.; Asadullah, L.K. Enhancement of adsorption efficiency of heavy metal Cu(II) and Zn(II) onto cationic surfactant modified bentonite. *J. Environ. Chem. Eng.* **2018**, *6*, 2821–2828. [[CrossRef](#)]
24. ElBastamy ElSayed, E. Natural diatomite as an effective adsorbent for heavy metals in water and wastewater treatment (a batch study). *Water Sci.* **2018**, *12*. [[CrossRef](#)]
25. Meng, Q.; Chen, H.; Lin, J.; Lin, Z.; Sun, J. Zeolite A synthesized from alkaline assisted pre-activated halloysite for efficient heavy metal removal in polluted river water and industrial wastewater. *J. Environ. Sci.* **2017**, *56*, 254–262. [[CrossRef](#)] [[PubMed](#)]

